IGNITOR Physics Assessment and Confinement Projections

W. HORTON[1], F. PORCELLI[2,3], P. ZHU[1], A. AYDEMIR[1], Y. KISHIMOTO[4], T. TAJIMA[1]

[1]Institute for Fusion Studies, The University of Texas, Austin, TX, 78712
[2]INFM and Dipartimento di Energetica, Politecnico di Torino, 10129 Torino, Italy
Plasma Science and Fusion Center, MIT, Cambridge, MA USA
[4]JAERI, Plasma Theory, Tokai-Mura, Naka-Gun, Ibaraki-Ken 319-11, JAPAN

Abstract

An independent assessment of the physics of Ignitor is presented. Ignitor is a physics demonstration experiment, with the main goal of achieving thermonuclear ignition, defined as the regime where fusion alpha heating compensates for all forms of energy losses. Simulations show that a pulse of α particle power up to 10-20 MW is produced for a period over a few seconds. Crucial issues are the production of peaked density profiles on a time-scale of several energy confinement times, the control of current penetration for the optimization of ohmic heating and sawtooth avoidance. The presence of a 10-20 MW Ion Cyclotron Radio frequency system and the operation of a high-speed pellet injector are considered essential to provide added flexibility in order to counter unexpected, adverse plasma behavior.

1 Introduction

IGNITOR [1, 2] is a physics demonstration experiment. Its main goal is to achieve thermonuclear ignition, defined as the regime where the fusion alpha heating compensates for the thermal energy losses due to anomalous transport and radiation. The purpose of this work is to provide an independent assessment of the capabilities of the IGNITOR tokamak machine. The relevant information that would be gained from such an experiment can be summarized as follows:

(i) Improved understanding of plasma turbulence and transport processes, by the exploration of high-plasma-density, high-magnetic-field regimes never accessed before. More specifically, IGNITOR would provide insight into the ohmic confinement scaling laws and self-organized plasma

profiles at high temperatures. Furthermore, it would provide relevant information on the conditions required for the spontaneous generation of plasma rotation through anomalous angular momentum transport. Plasma rotation is believed to play an important role in determining the level of turbulent fluctuations.

(ii) Alpha particle physics issues, in particular: alpha particle confinement, collective electromagnetic modes excited by the fusion alphas, and the nature of alpha particle heating. We note that an outstanding alpha physics issue is whether collective instabilities excited by the fusion alpha particles, such as fishbones and Toroidal Alfvén Eigenmodes (TAE), can seriously degrade the quality of confinement. A second outstanding physics issue is whether alpha particle heating causes the same degree of confinement degradation as other forms of auxiliary plasma heating.

(iii) The control of a fusion burning plasma over physically significant time scales. With a current flat top of a few seconds, IGNITOR should have a long enough pulse-length to thoroughly examine alpha particle physics and thermal transients associated with the DT burn.

(iv) The IGNITOR experiment would give first indications about a possible development path to tritium-poor, reduced neutron production of fusion power.

Ignition in IGNITOR would be reached under non-steady-state conditions as in fact ignition is intrinsically a time evolving event. The ignited regime would last a few confinement times ($2-5\tau_E$, $\tau_E \sim 0.5s$) and many alpha particle slowing down times ($50-100\tau_{sd}$), which is adequate from the physics point of view.

The concept of ignition is defined [3] as the plasma state where the heating power due to the fusion alpha particles compensates for all forms of power losses (due to anomalous transport and radiation). It is worthwhile to discuss this concept quantitatively, especially in view of non-steady-state operation. Consider the power balance equation,

$$\frac{dW}{dt} = P_{\rm ohm} + P_\alpha + P_{\rm aux} - P_{\rm loss}, \tag{1}$$

where W is the plasma energy content, $P_{\rm ohm}$ is the ohmic power, P_α is the alpha particle heating

power, $P_{\rm aux}$ is the auxiliary heating power, and $P_{\rm loss}$ is the loss power, including radiation losses. In the ignited state, $P_\alpha = P_{\rm loss}$ and the auxiliary power, $P_{\rm aux}$, may be switched off. Thus, ignition is an overheated state with $dW/dt = P_{\rm ohm} > 0$. One may introduce a parameter $Q^* = P_{\rm fus}/(P_{\rm loss} - P_\alpha)$ where the fusion power is given as $P_{\rm fus} = (17.6{\rm MeV}/3.5{\rm MeV})P_\alpha \simeq 5P_\alpha$ for a D-T reacting plasma. With this definition, $Q^* = \infty$ at ignition. Alternatively, using the power balance relation, one may write

$$Q^* = \frac{P_{\rm fus}}{(P_{in} - dW/dt)}, \tag{2}$$

where $P_{in} = P_{\rm ohm} + P_{\rm aux}$. A key objective of IGNITOR is to provide multi-megawatts of Ohmic power and to minimize the external symmetry breaking auxiliary power $P_{\rm aux}$. A key objective of IGNITOR is to provide multi-megawatts of Ohmic power and to minimize the external, symmetry-breaking auxiliary power $P_{\rm aux}$.

The parameter Q^* is the measure of fusion power to the input power, taking into account the transient loading/unloading of plasma energy, $W(t)$. One can see that Q^* becomes equal to the widely used thermonuclear gain parameter, $Q = P_{\rm fus}/P_{in}$, when $dW/dt = 0$, i.e. Q^* is the natural extension of Q under non-steady-state operation. During transient regimes, the difference between Q and Q^* becomes important and should be kept in mind. For instance, for the simulation example in the first column labeled Coppi of Table I of an ignited discharge in IGNITOR, one finds $Q^* = \infty$, while $Q = 8.6$. Table I gives the parameters of IGNITOR, a simulation from Ref. [1] of the IGNITOR team in the first column, and two times called the cross-over point (second column labeled COP) and a burning plasma (third column labeled BP) from the first simulation discussed in this new work.

IGNITOR belongs to a family of high-field tokamak experiments, pioneered by the Alcator machine at MIT in the 1970s and continued by the Alcator C/C-Mod and the Frascati FT/FTU series of experiments. A full assessment of plasma performance in these experiments is beyond the scope of the present work. It is noted, nevertheless, that a record value of $n_0\tau_E \sim 1 \times$

$10^{20} m^{-3}$ s was reached in ALCATOR C experiments with high peaked density, $n_0 \approx 2 \times 10^{21} m^{-3}$ and a confinement time of about 0.05 s.

Experience from ALCATOR C-MOD [4] and from FTU [5] indicates that the worst-case discharges in these machines have a confinement time that follows the ITER89P L-mode scaling, both in ohmic and with auxiliary heating at relatively high densities, while the neo-Alcator scaling is followed at lower densities. Regimes of improved confinement at high plasma density have been observed. H-modes have been observed in limiter as well as divertor configurations, in ohmic as well as in auxiliary heated discharges. Enhanced confinement in L-mode operation, such as the Improved Ohmic Confinement (IOC) regime observed in ASDEX-U [6], has also been observed in Alcator C [7] at relatively high density in plasmas with peaked density profiles. Recently [8], pellet-assisted ohmic discharges with very good confinement have been obtained in FTU, with a line-average density $\overline{n}_e \approx 4 \times 10^{20} m^{-3}$ and $\tau_E \approx 0.1$ s.

In IGNITOR, as compared with the record Alcator C experiments, a value of τ_E higher by about a factor of ten is needed to reach the target value $n_0 \tau_E \geq 4 \times 10^{20} m^{-3}$ s. This factor is only about five if the comparison is made against the recent FTU results.

We note, however, that high-field, high current operation in existing experiments has been limited. As a result, the available data bank is rather poor. It would be desirable to extend the database to more Ignitor-relevant demonstration discharges in order to increase the margin of confidence for extrapolations to Ignitor.

2 IGNITOR operational flexibility

Tokamak plasmas are complex physical systems. As such, it is generally accepted that our confidence in accurate quantitative predictions of plasma behavior in future tokamak experiments is limited. The IGNITOR device is designed to have the operational flexibility to explore new plasma regimes that will most likely appear with unforeseen plasma behavior. The flexibility of the IGNITOR experiment is related to:

Table I: Parameters of IGNITOR for a typical inductive operation scenarios. The first column is from Ref. [1]. The second column (COP) is the cross-over point where $P_\alpha \simeq P_{OH}$ at $t = 4.8\,$s and the third column (BP) is at $t \simeq 6\,$s in the burning plasma.

Parameter	Ref. [1] Coppi	COP	BP
R/a(m/m)	1.32/0.47	1.32/0.46	1.32/0.46
B_T(T)	13	13	13
I_p(MA)	11	12	12
κ_x/δ_x	1.83/0.4	1.83/0.4	1.83/0.4
q_a	3.5	3.5	3.5
β_p	0.26	0.11	0.16
$\beta_T\%$	1.2	1.6	2.3
β_N	0.67	0.71	0.99
$\langle n_e \rangle\,(10^{20}/\mathrm{m}^3)$	5	8.9	9.2
$\overline{n}_e$	6.2	8.9	9.6
$n_e(0)$	9.5	8.3	9.7
n_e/n_{GW}	0.4	0.5	0.5
$T_e(0)$(keV)	11.5	12.0	18.9
$T_i(0)$(keV)	10.5	10.8	15.5
P_{OH}(MW)	11	9.8	7.1
P_{ICRH}(MW)	0	0	0
P_{NBI}(MW)	0	0	0
P_α(MW)	19	10	31
P_{BREMS}(MW)	4	12	17
dW/dt(MW)	11	4.8	4.4
W_{th}(MJ)	12	15	20
$Q(Q^*)$	8.6(∞)	5.1 (10)	21.8 (57)
Z_{eff}	1.2	1.1	1.1
$\tau_E(s)$	0.62	0.73	0.52
$n\tau_E(10^{20}\,\mathrm{m}^{-3}\,\mathrm{s})$	6.0	6.5	4.8
$H_{97\mathrm{L}}$	1.3	1.1	1.4

(i) Its ability to explore a wide range of plasma densities and currents;

(ii) The operation of a high-speed pellet injector for the control of plasma profiles and for the exploration of enhanced confinement regimes.

(iii) The presence of a 18-24 MW Ion Cyclotron Radio Frequency system capable of providing additional heating, thereby affecting the current density evolution, and also capable of producing a suprathermal minority ion population for the control of MHD instability and for the simulation of alpha particle behavior. For instance, ICRH can be applied to relatively low-density regimes, in which the plasma temperature can be raised to values considerably higher than the optimal values for ignition, to attain the desired ratios of fast particle pressure relative to the plasma pressure.

(iv) A highly flexible poloidal field coil system, able to produce a considerable variety of equilibrium configurations. This includes the possibility of producing magnetic X-point configurations as an added tool for the investigation of enhanced confinement regimes.

3 Transport considerations

The study of plasma transport is one of the outstanding problems in fusion research. Following Kadomtsev [9]:

> *At the beginning of tokamak research there was the hope that experiments would allow us to determine empirical expressions for the relevant transport coefficients, which would then be explained theoretically. This hope was supported for a decade by results from small and medium size tokamaks, which suggested that the ion thermal conductivity was close to the neoclassical value. As for electrons, there was hope that experiments might help to produce a universal formula applicable to all cases. Understanding of confinement deepened in the 80s partially as a result of more detailed investigations in medium-size tokamaks, but mainly as the result of the operation of the new generation of large size tokamaks. A new understanding has emerged as a result of the discovery of various confinement regimes.*

It has become evident that self-consistent coupling of the turbulence with the plasma profiles plays a crucial role in the determination of the effective transport coefficients. Due to the feedback loops within this complex dynamical system, bifurcations arise analogous to those well known in turbulent neutral fluids. Thus, there are a variety of plasma confinements states. In some cases similar system control parameters result in discharges that take different confinement paths. A well-known example occurred for the matched discharges in TFTR, in which one ultimately deviates from the other through the bifurcation to a new state known as Enhanced Reversed Shear (ERS) confinement [10]. These issues of plasma confinement are of fundamental importance to plasma science and can be addressed in fusion-grade plasmas with IGNITOR.

The IGNITOR team bases its confinement predictions on a combination of empirical and theoretical 1-D flux-surface-averaged transport models [2]. While such 1-D models are intellectually appealing, the unfortunate reality of tokamak physics is that we do not have a generally valid model of transport.

The confinement issue for IGNITOR should be addressed with various methodologies and from many different perspectives in order to make sure that the confinement will be sufficient for the ignition objective. In this paper, we first examine the predictions based on empirical scaling laws. Next, we discuss the possibility of enhanced confinement regimes. Finally, we examine heat diffusivity models and present our own 1-D simulations of Ignitor discharges.

A. Confinement time based on L-mode scaling laws

A good description of the L-mode database with approximately 3000 entries is given by the ITER-97 L-mode formula [11]:

$$\tau_E^{\mathrm{L97}} = 0.023\kappa^{0.64} R^{1.83} A^{0.06} B_T^{0.03} \overline{n}_e^{0.4} m_{\mathrm{eff}}^{0.2} I_p^{0.96} P_{\mathrm{loss}}^{-0.73}, \tag{3}$$

where $P_{\mathrm{loss}} = P_{in} + P_\alpha - dW/dt$ is the loss power, which includes radiation losses, and $P_{in} = P_{\mathrm{OH}} + P_{\mathrm{aux}}$. At ignition, $dW/dt = P_{in}$ and $P_{\mathrm{loss}} = P_\alpha$. For the reference case of Table I, $P_{\mathrm{loss}} =$

19 MW at ignition. Taking the remainder of the parameters from Table I gives $\tau_E^{97L} = 0.47\,\mathrm{s}$; thus to obtain the required confinement time of $\tau_E \approx 0.62\,\mathrm{s}$, an H factor of 1.3 would be required. Similarly if the older L-mode scaling expression ITER89-P scaling is used, then $\tau_{\mathrm{E89L}} = 0.4\,\mathrm{s}$ and an H factor of 1.55 is required.

The L97 scaling law has been compared with confinement in Tore Supra [14]. The Tore Supra database has 50 discharges with Fast Wave ICRH that deposits its energy into the electrons, $P_{\mathrm{ICRH}} = P_0 \exp(-r/L_p)$, in a highly localized core with $L_p \approx a/5$. Thus, the fast wave ICRH heating is a rough simulation of the alpha power heating to the electrons. In addition, Tore Supra operates routinely in L-mode and exhibits various levels of enhancement over the ITER-97 L-mode scaling law as a function of density profile peaking. Thus, even though not a high field tokamak, Tore Supra is relevant to IGNITOR considerations. The best discharges have an enhancement factor of H =1.4 to 1.7 with respect to the ITER-97-L mode formula, which should be a conservative calculation of τ_E.

A key scientific issue that IGNITOR would address is whether the ohmic power at multi-megawatt levels plays the same role as P_{aux} in the confinement scaling laws as assumed in the above estimate of the confinement time. The same kind of question arises for the alpha heating power since this would become the dominant form of heating in IGNITOR.

B. Improved confinement regimes with peaked density profiles

Since the IGNITOR proponents suggest that ignition may be reached with ohmic heating only, it is convenient to start our discussion with the consideration of ohmic confinement modes. As is well known, the LOC (linear ohmic confinement) mode is a regime of ohmic confinement where a linear relationship between energy confinement time and density, i.e. neo-ALCATOR scaling, is valid [15]. The LOC regime corresponds to the best confinement mode. Unfortunately, at regular conditions with increasing density, the LOC regime makes a transition either into a saturated ohmic confinement (SOC) mode or into the L-mode with Goldston confinement scaling. The

critical density at which the transition between LOC and SOC regimes occurs is the so-called Shimomura density [16], whose expression is

$$n_s \approx (A_i/2)^{1/2} B_T/Rq_\psi \tag{4}$$

where A_i is the mean atomic mass number, B_T is expressed in Tesla, R in meters and n_s in $10^{20}m^{-3}$.

Different improved confinement regimes look like a LOC mode extended into the high-density region with subsequent saturation. One such improved confinement mode, the H-mode, will be discussed in Subsec. 3D. Here, we consider improved confinement regimes that can be reached with peaked density profiles. These regimes are listed as follows:

(i) The improved ohmic confinement (IOC) mode, initially discovered in ASDEX [6].

(ii) The radiative improved (RI) mode, discovered in TEXTOR [17].

(iii) The P-mode, which is a mode of improved ohmic confinement both in ohmic and in auxiliary heated discharges, first obtained with the help of pellet injection in ALCATOR-C [7].

(iv) The supershot, or S-mode, experimentally discovered in TFTR with central neutral beam injection (NBI) and strongly peaked density distributions [18].

(v) Fast Wave ICRH on Tore Supra [19, 14]

In the experimental regimes listed above, energy confinement enhancement factors up to 2-3 over that for L-mode have been obtained. Clearly, the relevant question is whether IGNITOR can access any of these regimes. Note that the key feature common to these improved confinement regimes is the realization of peaked density profiles. Different methods and considerable operational skills in the four tokamaks mentioned above have achieved this. In ASDEX, peaked densities and the IOC mode were obtained after appropriate wall conditioning and decreased gas puffing. In TEXTOR, the transition from the L to the RI mode was obtained with impurity seeding. In this way, a strongly radiating layer was established at the edge, with a corresponding decrease of the edge temperature and a steepening of the density gradient deeper inside the

plasma. In ALCATOR-C, pellet deposition in the plasma core resulted in peaked density profiles and the establishment of the P-mode. In TFTR, peaked densities were obtained in supershots with central NBI deposition.

More recently, a spontaneous density profile peaking has been observed in Alcator C-MOD H-mode plasmas at the H to L transition when the the additional ICRH resonant layer was placed well onto the high field side. Density peaking has also been observed in the same device during Ohmic H-modes when the toroidal field was ramped down. These phenomena are not fully understood and are under experimental investigation, with the objectives of extending the duration of the high performance phase and attempting to simultaneously increase the temperature and density peaking, possibly with the aid of pellets and multiple resonance ICRH.

Recent experiments [8] with high fields and pellet injection have been carried out by the FTU machine in Frascati. Estimated confinement times of about 90-100 msec have been reached with a magnetic field $B \approx 7T$, a line-average density $\overline{n}_e \approx 4 \times 10^{20} m^{-3}$ (the measurement of the density profile is not available at present) and a current $I_p \approx 0.8\,\mathrm{MA}$. The improvement in confinement lasts for more than one confinement time and it is recovered after the injection of a second pellet. More experiments are planned in order to improve both the confinement time the neutron yield, and to extend the duration of the high confinement regime, presently limited by core MHD activity.

From a theoretical viewpoint, peaked density profiles are known to have a beneficial effect on plasma confinement through the quenching of the ion temperature gradient (ITG) driven turbulence. Peaked density profiles reduce the two dimensionless profile parameters, η_i and η_e, that represent driving terms for the instability of ion and electron temperature gradient modes and their associated plasma turbulence for peaked density profiles. For flatter density profiles, the ITG stability condition is that L_{Ti}/R exceed a critical value, which is typically not compatible with the overall required temperature difference between the edge and core plasmas. In the 80s, several theoretical investigations of ITG modes supported the conclusion that the improved

confinement in Alcator C pellet fueling experiments [7] was correlated in time with the drop of the η_i parameter. Numerous other machines have shown discharges with improved confinement from density peaking. For instance, Ref. [20] predicts a suppression of the ion thermal flux due to ITG turbulence going from L-mode to the RI-mode in TEXTOR [21, 22]. As far as the electron temperature gradient driven turbulence is concerned, there are two theoretical forms of the anomalous electron thermal diffusivity that are depressed by high density: the dissipative trapped electron turbulent diffusivity and the short wavelength electromagnetic diffusivity with mixing length proportional to the collisionless skin depth [14, 23].

In IGNITOR, ignition would be reached with densities well below the Greenwald density limit, which must be considered as a distinct advantage. However, density peaking is crucial to gain access to improved confinement regimes. Strong density peaking in IGNITOR depends on the existence of an inward particle pinch. There are two theoretical models used to explain the particle pinch that occurs in tokamaks. The classical mechanism known as the Ware pinch is the off-diagonal transport coefficient that is conjugate through symmetries to the experimentally verified bootstrap current. While no clear experimental verification exists for the Ware pinch, an inward convection is required for transport modeling to be consistent with the measured density profiles. The density pinch effect is also modeled through drift wave turbulence driven by the temperature gradients, where again symmetries dictate an off-diagonal transport matrix producing a turbulent inward particle transport [24].

As discussed in Sec. 6, IGNITOR has adopted the cold radiating mantle solution, which may turn out to be advantageous for the formation of peaked density profiles. Indeed, the qualifier radiative in the RI-mode refers to the fact that this mode was discovered in TEXTOR while the cold plasma mantle concept was being established as a feasible means to solve the reactor exhaust problem [25]. Modeling the density profile with the RITM code has shown that an essential ingredient for peaking of the density profile is the action of the radiative mantle on the anomalous inward pinch velocity v_{in}, which is taken to have the form $v_{in} = 1/(2T_e)(dT_e/dr)D$, where D is

the radial particle diffusivity. This form may be justified by arguments of profile consistency, but more generally as a fundamental off-diagonal contribution of the transport matrix for fluctuation-driven particle transport [26]. It was also found to be essential in explaining the SOC-IOC transition in ASDEX [27].

The question of the degree of profile control by high-speed pellet injection, which translates to the question of the penetration of the pellet particles in high-density plasmas, thus becomes a crucial issue for the IGNITOR project. Possible solutions for how to inject pellets from the high field side and facilitate pellet penetration must be investigated. Control of the plasma edge density during start-up and current flat top is also important, since it regulates the current penetration rate, as well as being related to the edge temperature.

C. Reversed magnetic shear modes

In the IGNITOR device, transient effects can be exploited to reach ignition in ohmically heated plasmas. When the current ramp is considered, the plasma current increases by adding skin layers on the outer surface of the plasma column. The current penetration time based on neoclassical resistivity is comparable to the pulse length time scale. As a consequence, non-monotonic q profiles may form during the current ramp and during a significant fraction of the current flat top. Since ignition is expected to be achieved near the end of the current ramp, IGNITOR is well suited for a Reversed Shear (RS) mode of operation [10] of the type observed in JET and in TFTR, among other devices. The PEP mode [28], which is the JET variant of the RS mode, was obtained with central ICRH and pellet injection. For these modes of operation, enhancement factors of H $\approx$ 2-3 can be achieved. The physics of confinement enhancement for a non-monotonic q profile clearly has basic differences with that in a monotonic q profile. It is possible that reversed magnetic shear is only one factor in achieving reduced turbulence, with sheared plasma rotation and/or peaked profiles also playing important roles. Thus, although non-monotonic q profiles may occur spontaneously in IGNITOR, the assistance of pellet injection

and ICRH in accessing enhanced RS regimes of operation seems rather important.

D. H-modes

H modes of operation normally require the presence of a magnetic X-point and heating power levels above a threshold value. The L-H power threshold formula recommended by the ITER-FEAT physics expert group is

$$P_{\rm LH}^{\rm IPB99(5)} = 3.24 \overline{n}_e^{0.62} B^{0.75} R^{0.98} a^{0.81} m_{\rm eff}^{-1}. \tag{5}$$

If an H mode is accessed, the ITER-FEAT ELMy H-mode scaling law predicts a confinement time according to the formula

$$\tau_E^{\rm IPB98} = 0.0562 \kappa^{0.78} R^{1.97} A^{-0.58} I_p^{0.93} B_T^{0.15} \overline{n}_e^{0.41} m_{\rm eff}^{0.19} P_{\rm loss}^{-0.69}. \tag{6}$$

For IGNITOR, these formulae give a power threshold

$$P_{\rm LH}^{\rm IPB98}({\rm IGNITOR}) \approx 19 \text{ MW}, \tag{7}$$

easily exceeded by a combination of ohmic and ICRH or alpha heating, and a confinement time at ignition

$$\tau_E^{\rm IPB98} = 0.98 \,{\rm s} \tag{8}$$

Again, the parameters of the examples in Eqs. (7) and (8) are from in Table I. With this value ($\tau_E = 0.98\,{\rm s}$) for the confinement time, there should be no problem to reach ignition in IGNITOR.

It is noted that the IGNITOR poloidal field system is capable of producing an X-point within the vacuum vessel, in which case IGNITOR has sufficient power for a transition to H-mode confinement. However, the IGNITOR first wall is not designed to handle the localized heat fluxes associated with divertor operation. Thus, standard H-mode operation is not desirable in IGNITOR.

On the other hand, H-mode quality plasmas have sometimes been obtained with the magnetic X-point outside the vacuum vessel. Indeed, H-modes have been observed in limiter configurations [29]. Furthermore, there is evidence from Alcator C-MOD of an enhanced L-mode with the magnetic X-point on the vacuum vessel wall [30]. In this case, the plasma is prevented from entering the H-mode by reversing the toroidal magnetic field so as to set the ∇B drift away from the single null divertor. For power thresholds well in excess of those that would be required for an L-H transition (if the ∇B drift were in the favorable direction), enhancement factors of 1.2-1.4 relative to L-mode have been obtained.

In all these cases, a more favorable, more uniform, heat flux distribution to the first wall may result. Thus, improved confinement assisted by X-point operation is a possibility worth exploring in IGNITOR, although at present the available experimental information is insufficient.

E. Heat diffusivities

Let us examine the question of confinement in IGNITOR from the point of view of the heat diffusivity value needed for ignition relative to models that are known to work well in other tokamak experiments.

i) JET plasmas are described by the Taroni-Bohm [31] model χ_e^{TB} and its extensions in the JETTO model.

$$\chi_e^{\mathrm{TB}} = 0.33 q^2 \left(\frac{-a \nabla p_e}{p_e} \right) \frac{T_e}{B} \tag{9}$$

ii) ITG formulas in the Multi-Mode Model (MMM) give the major contribution to the total anomalous thermal diffusivity. The fluid model by Nordman and Weiland [57, 58] is implemented for that part of the Multi-Mode model for the transport by ITG mode. The ITG mode growth rates numerically computed from the Weiland model are then used to estimate the fluctuation level with the quasilinear approximation. The anomalous transport coefficients, which are functions of the fluctuation level, are thus obtained for ITG modes in the Multi-Mode model. Similar models for resistive-ballooning and kinetic-ballooning modes are included in the MMM

model [34].

iii) the electrostatic (ES) turbulent electron transport

$$\chi_e^{\rm es} = C_e^{\rm es}\, q^2 \left(\frac{R}{L_{T_e}}\right)^{3/2} \left(\frac{\rho_e^2 v_e}{T_e}\right) \left(|\nabla T_e - (\nabla T_e)_c|\right) \tag{10}$$

where

$$(\nabla T_e)_c \simeq 1.88 \left(\frac{|s| T_e}{qR}\right) \left(1 + Z_{\rm eff}\, \frac{T_e}{T_i}\right) \tag{11}$$

and

iv) the electromagnetic (EM) turbulent electron diffusivity, based on electromagnetic turbulence driven by ETG and collisionless electron skin depth [9]

$$\chi_e^{\rm em} = C_e^{\rm em}\, \frac{qc^2}{\omega_{pe}^2 \left(L_{T_e} R\right)^{1/2}} \left(|\nabla T_e - (\nabla T_e)_c|\right). \tag{12}$$

Formulae (13)-(15), with $C_e^{\rm es} = 0.05$ and $C_e^{\rm em} = 0.1$, show good predictive/interpretative performance for the electron power balance in Tore Supra [19, 14].

4 Transport Simulation Results with JETTO and MMM95

The range of predictions for IGNITOR performance may be assessed by comparing the results of the empirical transport models of Taroni-Bohm and the mixed Bohm-GyroBohm (Erba *et al.* 1998 [32]) contained in JETTO with the multiple mode model MMM95 (Bateman, 1998 [33]).

We have run these codes in standard configurations which do not include off-diagonal particle pinch terms nor pellet injection. The only fueling is from the edge and thus to obtain the required average density the edge density is too high at approximately 75% of the core density. In order to adjust for the lack of peaked density profiles, the line-averaged density values we use in the simulations (see columns 2 and 3 of Table I), while still significantly lower than the Greenwald density limit, are higher than the nominal IGNITOR values reported in the first column of the same table. In future simulations we will investigate how much change in performance can be

obtained with density profile control. In these codes the pedestal temperature must be supplied: for the reference value we use 2 kev. We note more optimistic values are reported for the FIRE experiment of 3.0 to 6.7 kev in a work [34] that compared edge predictions for ITER, AIRES-RS and FIRE. We acknowledge that several aspects of the present IGNITOR modeling are not as faithful to the IGNITOR concept as those reported early by the IGNITOR team.

The first simple model is a thresholdless parameterization defined as Taroni-Bohm

$$\chi_e^{\mathrm{TB}} = \alpha_B \frac{q^2(r)a}{B_T}\left(-\frac{dT_e}{dr}\right) \tag{13}$$

along with an additional gyro-Bohm contribution where the constant α_B is calibrated with certain JET discharges and validated on other discharges. The model has good predictive power for JET, TS and JT60U. The theoretical basis from particle-in-cell simulations is given in Kishimoto *et al.* [35] and Furnish *et al.* [36] for Bohm scaling. The power balance of $P_L = q_r^{\mathrm{TB}} S = P_{\mathrm{aux}}$ with the heat flux q_r and surface area $S = 4\pi^2 Rr$ from Eq. (10) leads to a global τ_E scaling exponents close to the ITER97L formula [11].

The multiple mode transport model (MMM95) gives consistently one of the best performances for the ITER profile databases. It contains descriptions of all the standard forms of plasma turbulence including resistive-ballooning, TEM, CTEM, and ITG. We have modified the code to include E_r-shear and reversed q-profile [37] but will not report on this MMM2000 version here. The MMM95-version is calibrated with circular TFTR discharges and tends to be strongly L-mode in character and thus is overly pessimistic for JET, JT60U, and DIII D. Thus, we expect these two models to bracket the performance.

The highest performance discharges are obtained with the mixed Bohm/gyro-Bohm model which is also called the JETTO model since it was first embodied in the JET transport code JETTO. Figure 1 shows the time traces of several key parameters in an Ohmic ignition discharge simulation. The time interval where $P_\alpha(t)$ raises above $P_{\mathrm{loss}} = W/\tau_E$ is $t_{ig} = 4-5\,\mathrm{s}$. After $t = 6\,\mathrm{s}$ the discharge is approaching a quasi-steady burning state with $Q^* = 5 \times (50\ \mathrm{MW})/(5\ \mathrm{MW}$ **Fig.1**

$+0_{\rm aux}) \simeq 50$ where $P_\alpha \approx 50$ MW and $P_\Omega \simeq 5\,$MW. To obtain the regime requires the current ramp shown in frame (a) from 7 MA to 12 MA in $\Delta t_{I_p} = 2\,$s and in frame (b) the density rise of $\langle n_e \rangle$ from $80 \times 10^{19}\,{\rm m}^{-3}$ to $\lesssim 100 \times 10^{19}\,{\rm m}^{-3}$ in the time interval $t_1 = 1\,$s to $t_2 = 6\,$s. In frame (c) we show the rising $P_\alpha(t)$ and falling $P_\Omega(t)$ and the sum of the total input power to the plasma heating $P_{\rm in} = P_\Omega(t) + P_\alpha(t)$. In frame (d) we show the rising plasma energy $W_{\rm tot}$ along with dW/dt which is the power associated with the increasing stored plasma energy. In frame (e) we show the two-type local energy confinement time $\tau_E(t) = W(t)/(P_\Omega + P_\alpha)$ and $\tau_E^*(t) = W(t)/(P_\Omega + P_\alpha - dW/dt)$. The radiated power is too small compared with the uncertainties in transport to warrant inclusion in $\tau_E(t)$. Frame (d) shows that the two definitions give the same basic descriptions except for the time interval around the ignition time $t_{\rm ig} \approx 4\,$s where there is a secular increase in the stored plasma energy $W(t)$. In the quasi-steady state there are fluctuations in $W(t)$ about a mean value that produce the sharp spikes in $\tau_E^*(t)$. In frame (f) the fusion gain parameters Q^* and Q are shown as functions of time, where Q^* approaches 40 to 60, signifying the occurrence of ignition. Fig. 2 shows the electron and ion temperature profiles in the quasi-steady state (e.g. at $t = 6.5\,$s). The core ratio is $T_e(0, 6.5\,{\rm s})/T_i(0, 6.5\,{\rm s})$= 21 keV/17 keV= 1.2. The edge temperatures are 2 keV. The gradients are of order $20\,$keV/m which is much less than the record gradients achieved at $I_p = 2 - 3\,$MA in large tokamaks. For example, JT60U#17110 reported at IAEA, 1993 and published in Ref. [12] achieve 70 keV/m for a period of several τ_E.

Fig.2

Tore Supra operates with $P_{\rm aux} \simeq 5 - 7\,$MW for periods of $2 - 5\,$s corresponding to time intervals of $100\,\tau_E \approx 2\,$s with RF power $\gtrsim 5\,$MW of core electron heating with $dT_e/dr \approx 10\,$keV/m. Thus, we expect these gradients can be maintained although they will probably drive ITG, TEM, and ETG turbulence. The exception would be if the density profile can be maintained as sufficiently peaked by pellet injection that $d\log T_{i,e}/d\log n_e \leq 1$ then ITG and ETG drives will be eliminated.

The evolution for the same current and density ramps for the ITG and TEM theory-based

transport model is shown in Fig. 3. Here the confinement time shown in frame (d) of Fig. 3 is **Fig.3** $\tau_E \simeq 0.6\,\mathrm{s}$, higher by $0.6/0.4 = 1.5$ than the ITER97L value of 0.4 s given in the TTP (Laval, 2000) CEA Report. Now frame (c) shows that $Q^*_{\mathrm{MMM95}} \simeq 5\times$(5MW)/(11 MW Ohmic)$\simeq$ 2.3 showing that auxiliary heating is necessary to achieve a successful ignition experiment with this theory-based transport model. In Fig. 4 we see the ITG turbulence limits $T_i \simeq 7$ keV and T_e is **Fig.4** tightly coupled to T_i by the high collisionality of this lower-temperature plasma.

4.1 Sawtooth effects

Here we show the sawtooth effects on the purely Ohmic discharges using both JETTO and MMM95 models. The JETTO case without sawtooth ignites and goes to a stable burn with $Q^* \approx 60$. The MMM95 case barely ignites. When the sawtooth is included in the simulations, both models predict no ignition. Then we show the results of adding 10 MW and 20 MW of RF heating and preheating power to the MMM95 model simulation to enhance the performance.

When the sawtooth is allowed in the simulations, Fig. 5a (JETTO model) and 5b (MMM95 **Fig.5** model) show that the increase of α heating power and the decrease of the Ohmic heating power stop at $t = 4\,\mathrm{s}$, the time at which the first sawteeth are triggered. After that time, the Ohmic heating power stays at high level while the α heating power remains at a very low level ($\sim 3\,\mathrm{MW}$), indicating no occurrence of ignition. The corresponding movements of the position of $q = 1$ surface is shown in Fig. 6a for both models. The two models give a similar description of **Fig.6a** the growth of the $q = 1$ radius $r_1(t)$ which saturates at $r_1/\overline{a} = 22\mathrm{cm}/64\mathrm{cm} = 0.34$ where $\overline{a} = \sqrt{\kappa}a = 64\mathrm{cm}$. The plasma pressure remains at or below the critical pressure $\beta_{p,c} \simeq 0.13$. Only one sawtooth model has been tried at this time. Due to the sensitivity to the sawteeth, we are now coding the Porcelli *et al.* [52] model. To better demonstrate the degrading effect of the sawtooth oscillation, we repeat the simulation with JETTO model in Fig. 1 but artificially turn on the sawtooth at $t = 6.5\,\mathrm{s}$, and plot out the time traces of Q^* and Q in Fig. 7. Both Q^* **Fig.7** and Q time traces immediately drop after $t = 6.5\,\mathrm{s}$, leaving the pulse of fusion power indicating

ignition before the sawtooth and its sharp determination after the sawtooth.

4.2 RF power scan

Now, we investigate the effect of auxiliary RF heating on the performance of IGNITOR. Simulations using JETTO model and MMM95 models with 10 MW and 20 MW of ion cyclotron RF heating powers applied from $t = 1.0\,\mathrm{s}$ to $t = 9.0\,\mathrm{s}$ are shown in Figs. 8 and 9. For the simulation using JETTO model, it can be seen in Fig. 8 that as the RF power increases, the **Fig.8** α heating power also increases, but the magnitude of sawtooth oscillation becomes larger at the same time. The fusion gain Q is around 2.2 as the plasma enters steady state beyond 4 s. Hence the overall improvement of the heating performance is not significant. For the simulation using MMM95 model in Fig. 9, the RF heating power is shown to have greatly increased the **Fig.9** α heating power until the sawtooth oscillation is triggered. Both Q^* and Q oscillate about the average value of 5 during the steady state. In simulations with both models, the RF heating is seen to enhance the magnitude of sawtooth oscillation. From Fig. 6b, which shows the position **Fig.6b** of $q = 1$ surface as the function of time for the 20 MW RF heating power cases, one can see the first major sawtooth occurs at $t \sim 3\,\mathrm{s}$ for the JETTO model while the first major sawtooth is not triggered until $t \sim 6\,\mathrm{s}$ for the MMM95 model. In this case, the growth of the $q = 1$ radius is strongly delayed in MMM95 model till 6s and then rapidly catches up with that of the JETTO model. The radius saturates at $r_1/\overline{a} = 26\mathrm{cm}/64\mathrm{cm} = 0.4$ and the plasma pressure well exceeds the theoretical estimate of $\beta_{p,c} \simeq 0.1 - 0.2$ for the ideal internal kink mode.

The simulations presented, while rudimentary, show that control (1) of the sawtoothing and the (2) density profile are critical elements for achieving the goal of ignition in IGNITOR. While these two problems have been identified earlier the simulations make quantitative the degree of the problem. By comparing predictions of an empirical-based transport model with a theory-based model, we highlight the problem of extrapolating from the present rather limited database in terms of high-field/high-density operations. We also see the need to use more advanced theory

models that incorporate the transport suppression from E_r-shear and from optimized magnetic shear current profiles.

The MMM2000 code includes the E_r and reversed magnetic shear turbulent suppression models. The code gives reasonable agreement with two OS-JET discharges and good agreement with two DIII-D negative central shear discharges [34]. Clearly, there is the expectation that the MMM2000 can yield higher performance than the L-mode confinement of MMM95. In contrast, the empirical formulas of JETTO and a new IGNITO-relevant database from the ITER global database give predictions for ignition to occur [38].

5 MHD stability and collective alpha particle modes

One of the main advantages of the IGNITOR experiment is the increased safety margin against MHD instabilities. The relatively low values of the plasma beta parameter and relatively large values of the safety factor needed at ignition guarantee this. Thus, IGNITOR should operate well below the stability thresholds for ballooning modes and for neoclassical tearing modes. Likewise, the incidence of disruptions in IGNITOR can be expected to be very low. A precise quantitative assessment of MHD stability requires further work.

The assessment of stability against internal kink modes, leading to the well-known sawtooth internal relaxation oscillations and fishbone oscillations, deserves a separate discussion. Here, the IGNITOR team has carried out a considerable amount of detailed work [2]. Indeed, it appears as if the ignition strategy in IGNITOR is partly driven by the necessity to avoid the deleterious effects of sawteeth. The transient nature of the approach to ignition is such that the q profile develop a $q = 1$ surface only well into the current flat top, after ignition is reached. In this way, the $q = 1$ radius, which measures the extent of the central plasma region affected by sawteeth, may be controlled. However, anomalous current penetration, for instance caused by double tearing modes, may lead to an early onset of sawtooth oscillations. The sawtooth model used here shows that with increasing $P_{\rm aux}$ the sawtoothing increases and significantly reduces

the fusion Q achieved.

Fishbone oscillations may be excited by the fusion alpha particles in IGNITOR. The relevant instability regime corresponds to modes oscillating at the thermal ion diamagnetic frequency [40]. Trapped alpha particles can resonate with these modes only at energies below 500 keV, i.e., only after they have deposited most of their energy in the plasma. The effect of fishbones on slowed-down alphas at these relatively low energies should be relatively mild. It is noted that the loss of slowed-down alpha particles may even be beneficial, as the deleterious effect of alpha ash accumulation would be reduced [39].

Since IGNITOR is designed to reach ignition at relatively low plasma temperatures,the projected alpha particle pressure is relatively low, in particular lower than the threshold for the excitation of Toroidal Alfvén Eigenmodes (TAE). However, operation at lower density and ICRH injection lead to higher plasma temperatures and higher alpha particle pressures, which could then allow for the experimental observation of TAE modes.

IGNITOR proposes to operate at such low poloidal beta that neoclassical tearing modes would only be very weakly excited, if at all. Also, even if they did occur they would probably grow too slowly to influence the approach to ignition. To the extent that a burning plasma regime is achieved and sustained for a time of the order of the skin diffusion time in IGNITOR, neoclassical tearing modes might be observed and studied. However, at the relatively high collisionality in IGNITOR, the threshold island width is likely to be quite high. Thus, neoclassical tearing modes seem to be of little concern for IGNITOR's basic mission.

6 Impurities

Another important advantage of the IGNITOR experiment is the expected high purity associated with high plasma density operation. The self-cleaning ability of high-density plasmas has been well documented by Alcator C-MOD [4] and FTU [41] experiments. A scaling law relating plasma purity, radiated power, and machine dimensions has been derived from a number of

experiments [42]. Based on these experiments, average Z_{eff} values of around 1.2 should be possible in IGNITOR. However, the problem of plasma purity is associated with the problem of reducing the power load on the first wall, where sputtering and evaporation produce impurities.

One possible solution to this problem is the divertor concept. While the IGNITOR poloidal system is capable of producing an X-point within the vacuum vessel, the IGNITOR first wall may not sustain the concentrated power load associated with divertor operation. Hence, the divertor solution appears impractical for IGNITOR.

The solution proposed by the IGNITOR team is the cold radiating mantle concept, with molybdenum tiles as the first wall material. In the high density regimes at which IGNITOR is expected to operate, strong screening of the main body of the plasma column from impurities has been observed. Recent experimental results [17] have indicated the possibility of operating with a radiating mantle able to dissipate up to 90% of the total power lost by the plasma without energy confinement degradation. Thermal loads in IGNITOR have been calculated for an ideal continuous first wall, under the conservative assumption that only 70% of the input power is radiated. Under normal operation, the maximum thermal load is estimated [1] to be 1.8 MW/m^2 with an average heat flux of less than 0.7 MW/m^2.

7 Conclusions

IGNITOR is essentially an ignition physics experiment, which is projected to bring a long-awaited demonstration of the scientific feasibility of magnetic fusion and pathway to study alpha particle and burning plasma issues. The main assets of IGNITOR are its high magnetic field and low beta, which increase safety margins with respect to MHD instabilities, and its expected high purity plasma. With high ohmic heating and supplementary ICRH, we find that it will be possible to access interesting regimes without relying on alpha particles and a highly irradiated environment. Thus, the physics exploration of confinement regimes and optimization could go far before the difficult ignition runs.

Any tokamak experiment in unexplored plasma domains should possess sufficient versatility to counter unexpected adverse behavior. IGNITOR flexibility lies in its ability to produce a wide range of plasma densities and currents and a variety of equilibrium configurations, including the capability of producing a magnetic X-point. The key to IGNITOR success, however, relies on adequate density profile control with the assistance of a high-speed pellet injector and adequate power injection from an ICRH system, capable of sustaining the plasma temperature at relevant values should ohmic scenarios fall short due to poorer than expected confinement properties. Pellets and ICRH would also allow relevant burn control studies at slightly sub-ignited states.

Our conclusion, drawn partly from the large knowledge base of earlier tokamak experiments and partly from the simulations presented here, is that ignition in limiter discharges is a distinct possibility in IGNITOR. Historically, we observe that the record values of the Lawson product $\overline{n}_e\tau_E$ and the clean (low $Z_{\rm eff}$) plasma achieved in purely Ohmic discharges clearly indicates an interest in experiments with 4-10 MW of Ohmic heating. Our simulation results are consistent with IGNITOR reaching ignition as shown in Table I. The success of IGNITOR relies importantly on accessing improved confinement regimes with an enhancement factor of about 1.4 over predictions of confinement time based on L-mode scaling laws. Improved confinement regimes, such as the IOC, RI, P and S confinement modes, may be accessed in IGNITOR, provided that peaked density profiles are produced. Again, pellet injection is expected to play an important role in this. Reversed Shear and PEP modes may also be realized, since non-monotonic q profiles may form during the transient approach to ignition. The control of current penetration, by means of appropriately ramping the current, density and plasma volume, is also crucial in order to optimize Ohmic heating and for sawtooth avoidance. H-modes are probably not desirable in IGNTIOR, given the high levels of localized heat flux to the first wall that would result. However, an appropriate use of the magnetic X-point may provide some degree of enhancement in L-mode type of behavior and the EDA type of edge mode may be useful to distribute the heat flux. It should be remarked, nevertheless, that transport in tokamak plasmas as well as sawteeth

are not fully understood and that predictions about fusion performance should be taken with caution.

8 Acknowledgments

This work was stimulated by discussions within the Thermonuclear Tokamak Panel during 1999-2000 convened by R. Pellat with the panel members J. Callen, G. Cordey, O. Gruber, J. Jacquinot, G. Laval, J.-F. Lucian. The authors also wish to thank G. Bateman, F. Bombarda, B. Coppi, M. Greenwald, J. Johner, A. Kritz, M. Ottaviani, M. N. Rosenbluth, L. Sugiyama, J. Van Dam, and A. Wootton for useful discussions.

This work was supported in part by the U.S. Dept. of Energy Contract No. DE-FG03-96ER-54346.

References

[1] B. Coppi, *et al.*, MIT (RLE) Report PTP 99/06 (1999).

[2] B. Coppi, M. Nassi, and L. E. Sugiyama, Physica Scripta **45**, 112 (1992).

[3] K. Miyamoto, *Plasma Physics for Nuclear Fusion*, (MIT Press, Cambridge, 1989), pp. 8-9

[4] M. Greenwald, *et al.*, Phys. Plasmas **2**, 2308 (1995).

[5] G. Bracco, *et al.*, in Proc. 21st EPS Conf. in *Plasma Physics and Controlled Fusion* (Montpellier, 1994), p. 70.

[6] M. Bessenrodt-Weberpals, K. McCormick, F.X. Söldner, *et al.*, The multiple facets of ohmic confinement in ASDEX, Nucl. Fusion **31**, 155 (1991).

[7] M. Greenwald, *et al.*, Phys. Rev. Lett. **53**, 352 (1984).

[8] D. Frigione, FTU, High density performance, International Atomic Energy Agency, Sorrento, Italy (2000).

[9] B. B. Kadomtsev, Tokamak Plasma: A Complex Physical System (IOP, Bristol, 1992).

[10] E. Mazzucato, S. H. Batha, M. Beer, M. Bell, *et al.*, Turbulent fluctuations in TFTR configurations with reversed magnetic shear, Phys.Rev. Lett. **77**, 3145 (1996).

[11] S. M. Kaye and the ITER confinement database working group, Nucl. Fusion **37**, 1303 (1997).

[12] Y. Koide, M. Kikuchi, M. Mori, S. Tsuji, S. Ishida, N. Asakura, Y. Kamada, T. Nishitani, Y. Kawano, T. Hatae, T. Fujita, T. Fukuda, A. Sakasai, T. Kondoh, R. Yoshino, and Y. Neyatani. *Physical Review Letters*, **72**, 3662 (1994).

[13] G. Laval, Thermonuclear Tokamak Panel Report, CEA, Paris, France (2001).

[14] W. Horton, P. Zhu, G. Hoang, T. Aniel, M. Ottaviani, and X. Garbet, Electron transport in Tore Supra with fast wave electron heating, Phys. Plasmas **7**, 1494-1510 (2000).

[15] B. Coppi and E. Mazzucato, Phys. Letts. A **71**, 337 (1979).

[16] Y. Shimomura, JAERI Report JAERI-M 87-080 (1985).

[17] R. R. Weynants, *et al.*, Nucl. Fusion **39**, 1637 (1999).

[18] D. M. Meade, *et al.*, 13th Int. Conf. on Plasma Phys. Contr. Fusion Research (Washington, D.C., 1990), vol. 1, p. 9.

[19] G. T. Hoang, C. Bourdelle, X. Garbet, T. Aniel, G. Giruzzi, M. Ottaviani, W. Horton, P. Zhu, and R.V. Budny, Electron transport and improved confinement on Tore Supra, International Atomic Energy Agency, Sorrento, Italy (2000).

[20] M. Z. Tokar, *et al.*, Plasma Phys. Contr. Fusion **41**, L9 (1999).

[21] U. Samm, G. Bertschinger, P. Bogen, *et al.*, Radiative edges under control by impurity fluxes, Plasma Phys. Contr. Fusion **35**, B167 (1993).

[22] J. Winter, *et al.*, Phys. Rev. Lett. **71**, 1549 (1993).

[23] W. Horton, Drift wave transport, Rev. Mod. Phys. **71**, 735 (1999).

[24] B. Coppi and C. Spight, Phys. Rev. Lett. **41**, 551 (1978).

[25] A. M. Messiaen, J. Ongena, U. Samm, *et al.*, Transport and improved confinement in high power edge radiation cooling experiments on TEXTOR, Nucl. Fusion **36**, 39 (1996).

[26] K. C. Shaing, Phys. Fluids **31**, 2249 (1988).

[27] G. Becker, Analysis of energy and particle transport and density profile peaking in the improved ohmic confinement regime, Nucl. Fusion **30**, 2285 (1990).

[28] M. Hugon, B.Ph. van Milligen, P. Smeulders, *et al.*, Shear reversal and MHD activity during pellet enhanced performance pulses in JET, Nucl. Fusion **31**, 33 (1992).

[29] See, e.g., H. Weisen, F. Hofmann, M.J. Dutch, *et al.*, Ohmic H-modes in the TCV tokamak, Plasma Phys. Contr. Fusion **38**, 1137 (1996).

[30] M. Greenwald, private communication.

[31] A. Taroni, M. Erba, F. Tibone and E. Springmann, Plasma Phys. Control. Fusion **36**, 1629 (1994).

[32] M. Erba, *et al.*, Nuclear Fusion, **38** 1013 (1998).

[33] G. Bateman, A. H. Kritz, J. E. Kinsey, A. J. Redd and J. Weiland, Phys. Plasmas, **5**, 1793 (1998).

[34] G.W. Hammett, W. Dorland, M.A. Beer, and M. Kotschenreuther, Potential methods for improving pedestal temperatures and fusion performance, PPPL-3360 (October 1999).

[35] Y. Kishimoto, T. Tajima, W. Horton, M. J. LeBrun, and J. Y. Kim, Phys. Plasmas **3**, 1289 (1996).

[36] G. Furnish, W. Horton, Y. Kishimoto, M. LeBrun, and T. Tajima, Phys. Plasmas, **6**, 1227 (1999).

[37] P. Zhu, G. Bateman, A. H. Kritz and W. Horton, Phys. Plasmas, **7**, 2898 (2000).

[38] B. Hu and W. Horton, "Influential Tokamak Databases from L-mode International Database", IFS Report # 904 (2000).

[39] B. Coppi and F. Porcelli, Fusion Technol. **13**, 447 (1988).

[40] B. Coppi and F. Porcelli, Theoretical model of fishbone oscillations in magnetically confined plasmas, Phys. Rev. Lett. **57**, 2272 (1986).

[41] M.L. Apicella, *et al.*, Nucl. Fusion **37**, 381 (1997).

[42] G. F. Matthews, *et al.*, J. Nucl. Mat. 241-243, 450 (1997).

[43] G. Saibene, R. Budny, A. V. Chankin, *et al.*, Comparison of core and edge characteristics of NB and ICRH ELMy H-modes in JET, Nucl. Fusion **39**, 1133 (1999).

[44] R. La Haye *et al.*, in Controlled Fusion and Plasma Physics 1997 (Proc. 24th Eur. Conf. Berchtesgaden, 1997), Vol. 21A, Part III, European Physical Society, Geneva (1997) 1121-1244.

[45] M.F.F. Nave, S. Ali-Arshad, B. Alper, *et al.*, MHD activity in JET hot ion H-mode discharges, Nucl. Fusion **35**, 409 (1995).

[46] G.T.A. Huysmans *et al.*, Proc. 24th EPS Conference on Controlled Fusion and Plasma Physics, Berchtesgaden, June 1997; Part IV, p. 1857.

[47] T.S. Taylor, *et al.*, in *Plasma Physics and Controlled Nuclear Fusion Research 1990* (Proc. 13th Int. Conf. Washington D.C., 1990) vol. 1, IAEA, Vienna (1991) p. 177; Y. Kamada,

et al., in *Fusion Energy 1996* (Proc. 16th Int. Conf. Montreal, 1996), vol. 1, IAEA, Vienna (1997) p. 247.

[48] Y. Kamada, Characteristics of and issues regarding combined H-modes, Plasma Phys Control. Fusion **38**, 1173-1188, (1996).

[49] D. J. Campbell, D.F.H. Start, J.A. Wesson, *et al.*, Stabilization of sawteeth with additional heating in the JET tokamak, Phys. Rev. Lett. **60**, 2148 (1988).

[50] M. N. Bussac, R. Pellat, D. Edery, and J. L. Soule, Internal kink modes in toroidal plasmas with circular cross-sections, Phys. Rev. Lett. **35**, 1638 (1975)

[51] H. Lütjens, A. Bondeson, and G. Vlad, Ideal MHD stability of internal kinks in circular and shaped tokamaks, Nucl. Fusion **35**, 1625 (1992).

[52] F. Porcelli, D. Boucher, and M. N. Rosenbluth, Model for the sawtooth period and amplitude, Plasma Phys. Contr. Fusion **38**, 2163 (1996).

[53] Z. Chang, *et al.*, Phys. Rev. Lett. **74**, 4663 (1995).

[54] H. Zohm, The physics of edge localized modes (ELMs) and their role in power and particle exhaust, Plasma Phys. Control. Fusion **38**, 1213-1223, (1996).

[55] T. Kammash, *Fusion Reactor Physics*, (Ann Arbor Science Publishing, 1975), Ch. 8.

[56] W. Horton and T. Kammash, Anomalously confined tokamak reactor, Nucl. Fusion **13**, 753 (1973).

[57] H. Nordman and J. Weiland, Phys. Fluids B **5**, 1032 (1993).

[58] H. Nordman and J. Weiland, Nucl. Fusion **32**, 1653 (1992).

FIGURE CAPTIONS

FIG. 1. Time traces of a) plasma current, b) line-averaged electron density, c) heating powers, d) total plasma energy, e) confinement times, and e) fusion gains in the simulation (run #a010) of the purely Ohmic heating of IGNITOR (no auxiliary heating) using JETTO transport model without considering sawtooth.

FIG. 2. Ion and electron temperature profiles at $t = 6.5\,\mathrm{s}$ in the simulation (run #a010) of the purely Ohmic heating of IGNITOR (no auxiliary heating) using JETTO transport model without considering sawtooth.

FIG. 3. Time traces of a) plasma current, b) line-averaged electron density, c) heating powers, and d) confinement times in the simulation (run #a011) of the purely Ohmic heating of IGNITOR (no auxiliary heating) using MMM95 transport model without considering sawtooth.

FIG. 4. Ion and electron temperature profiles at $t = 6.5\,\mathrm{s}$ in the simulation (run #a011) of the purely Ohmic heating of IGNITOR (no auxiliary heating) using MMM95 transport model without considering sawtooth.

FIG. 5. Time traces of Ohmic and α heating powers in the simulation of the purely Ohmic heating of IGNITOR (no auxiliary heating) with sawtooth using a) JETTO model (run #a009) and b) MMM95 model (run #a007).

FIG. 6. Time traces of the $q = 1$ radii at sawtooth crash in the simulations with a) pure Ohmic heating and b) 20 MW auxiliary RF heating.

FIG. 7. Time traces of fusion gains Q^* and Q in simulation using JETTO model where sawtooth is turned on at $t = 6.5\,\mathrm{s}$.

FIG. 8. Time traces of a) Ohmic heating powers and b) α heating powers in the simulations of IGNITOR with 0, 10 MW and 20 MW RF heating powers, using JETTO model.

FIG. 9. Time traces of a) Ohmic heating powers and b) α heating powers in the simulations of IGNITOR with 0, 10 MW and 20 MW RF heating powers, using MMM95 model.

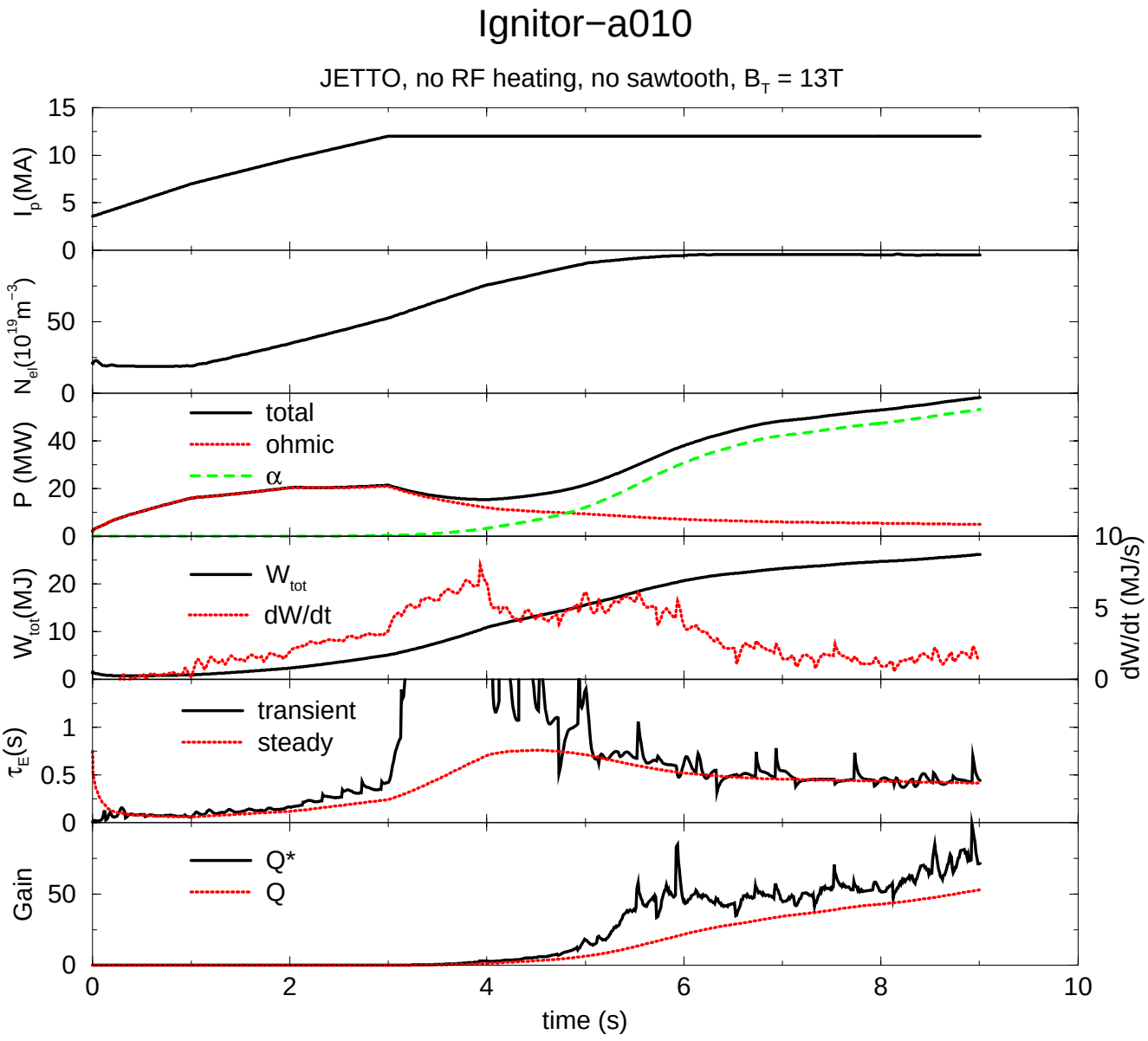
Ignitor−a010
JETTO, no RF heating, no sawtooth, B_T = 13T
I_p(MA)
N_el(10^19 m^-3)
P (MW)
total
ohmic
α
W_tot(MJ)
W_tot
dW/dt
dW/dt (MJ/s)
τ_E(s)
transient
steady
Gain
Q*
Q
time (s)

Fig.1

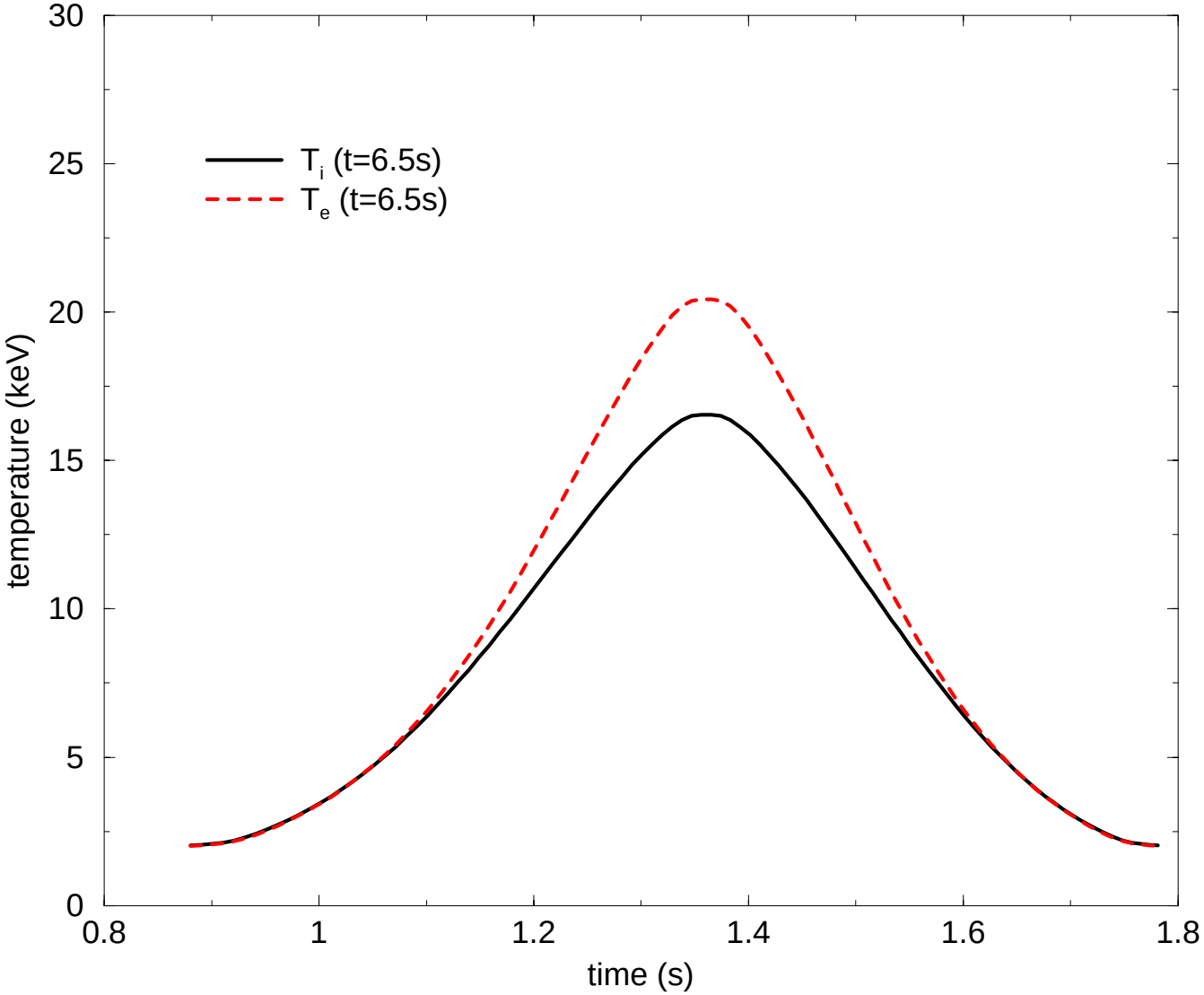
30
25
20
15
10
5
0
0.8
1
1.2
1.4
1.6
1.8
temperature (keV)
time (s)
T_i (t=6.5s)
T_e (t=6.5s)

Fig.2

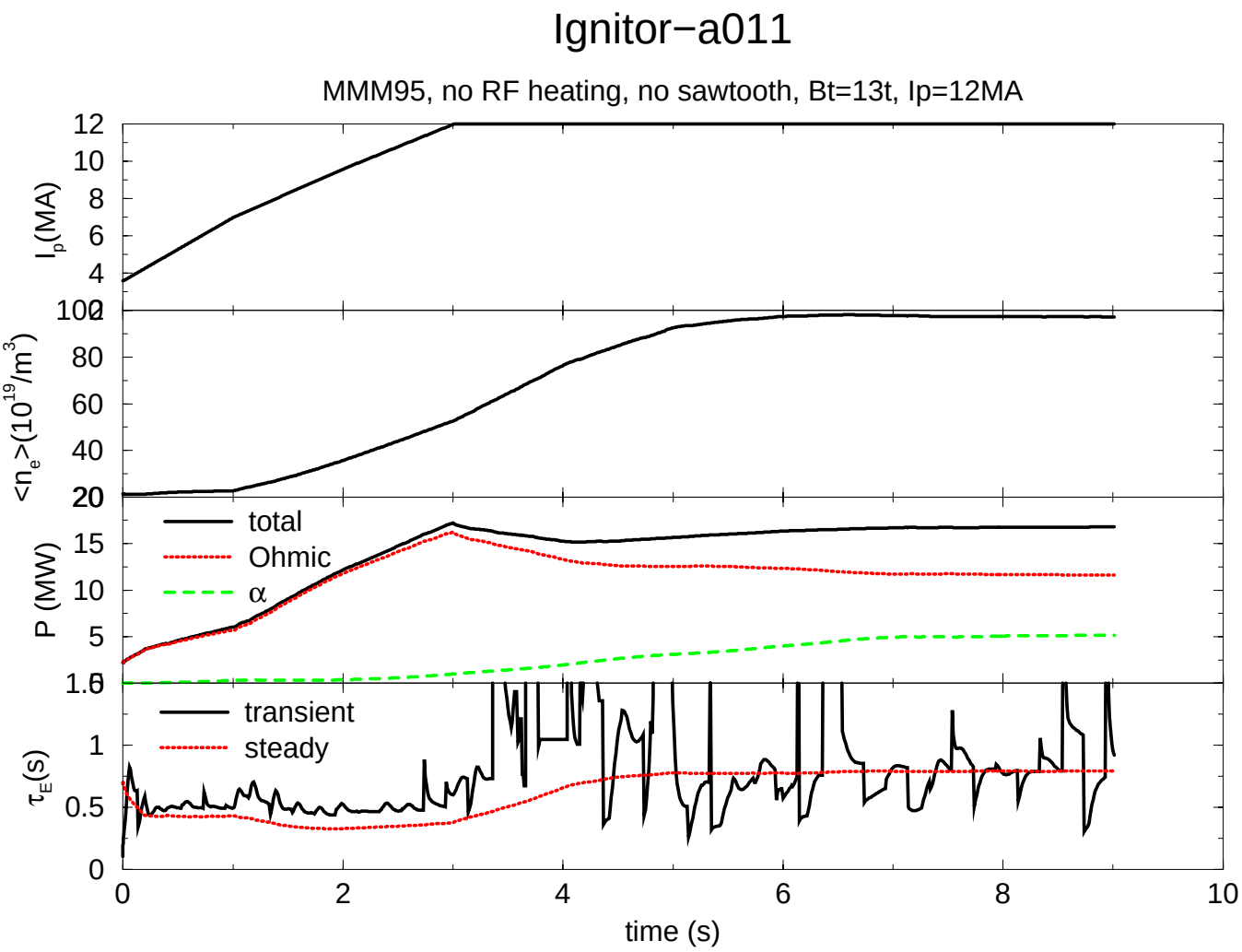
Ignitor−a011
MMM95, no RF heating, no sawtooth, Bt=13t, Ip=12MA
I_p(MA)
<n_e>(10^19/m^3)
P (MW)
total
Ohmic
α
τ_E(s)
transient
steady
time (s)

Fig.3

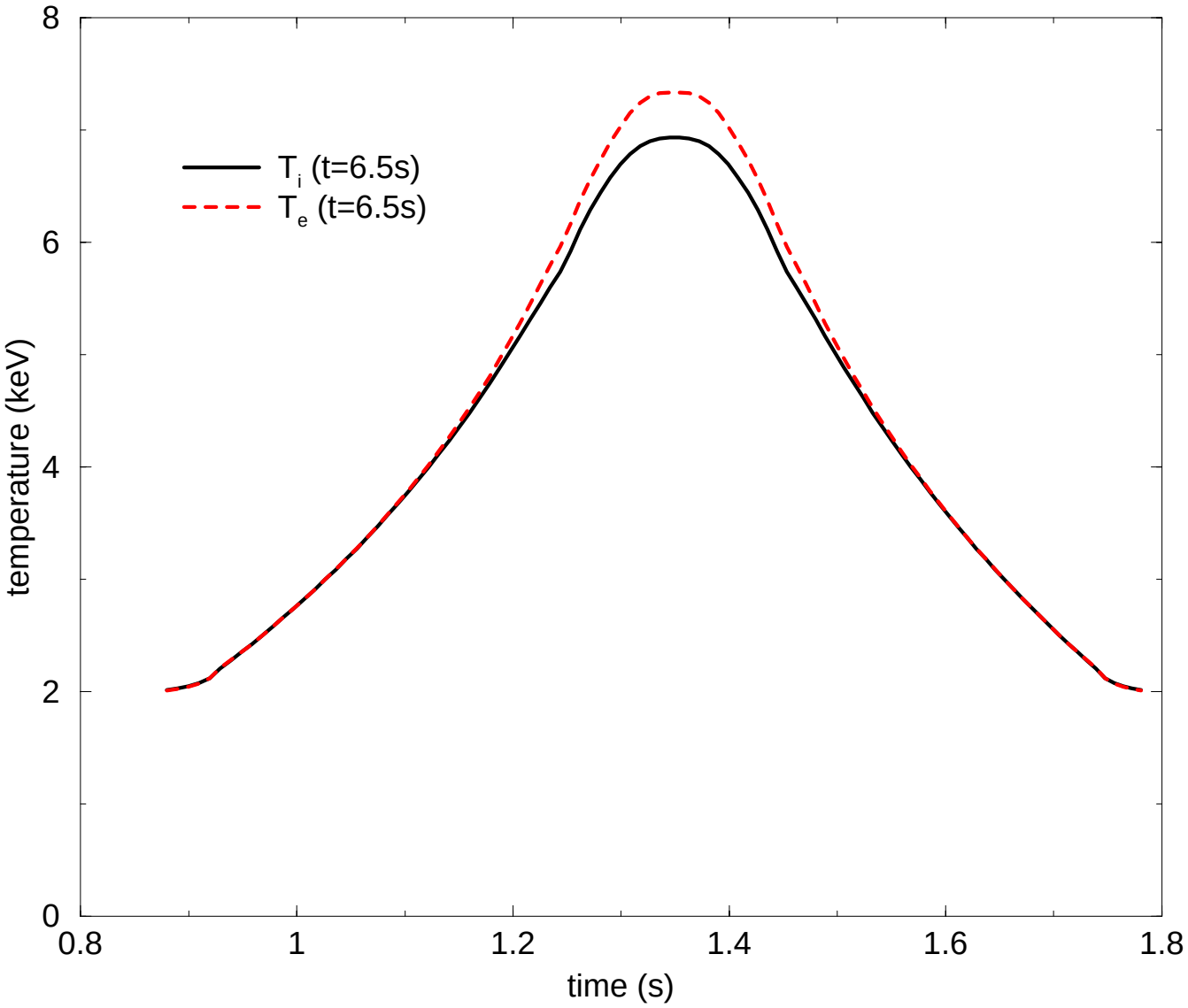

Fig.4

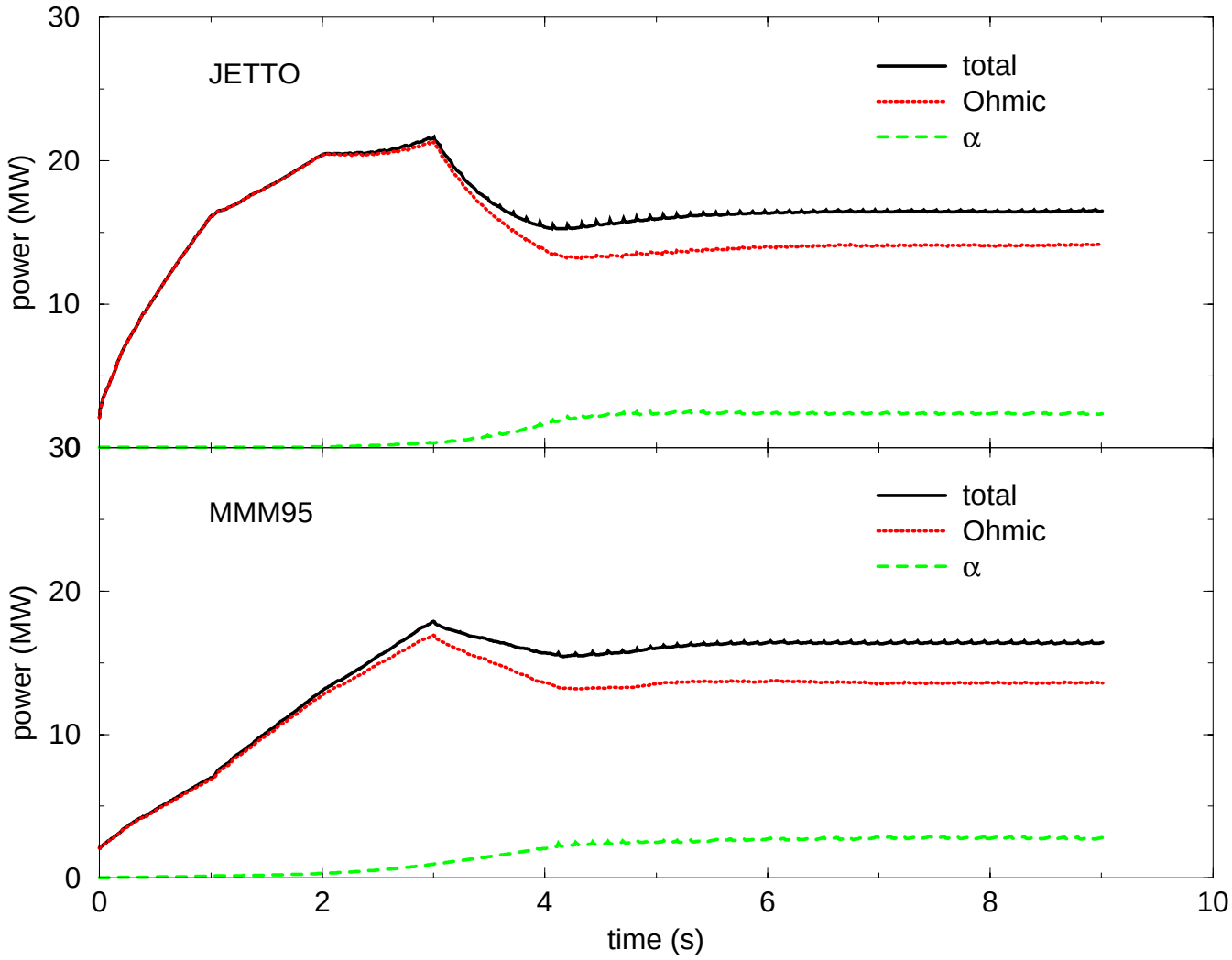
JETTO
total
Ohmic
α
power (MW)
30
20
10
0
MMM95
total
Ohmic
α
power (MW)
30
20
10
0
0
2
4
6
8
10
time (s)

Fig.5

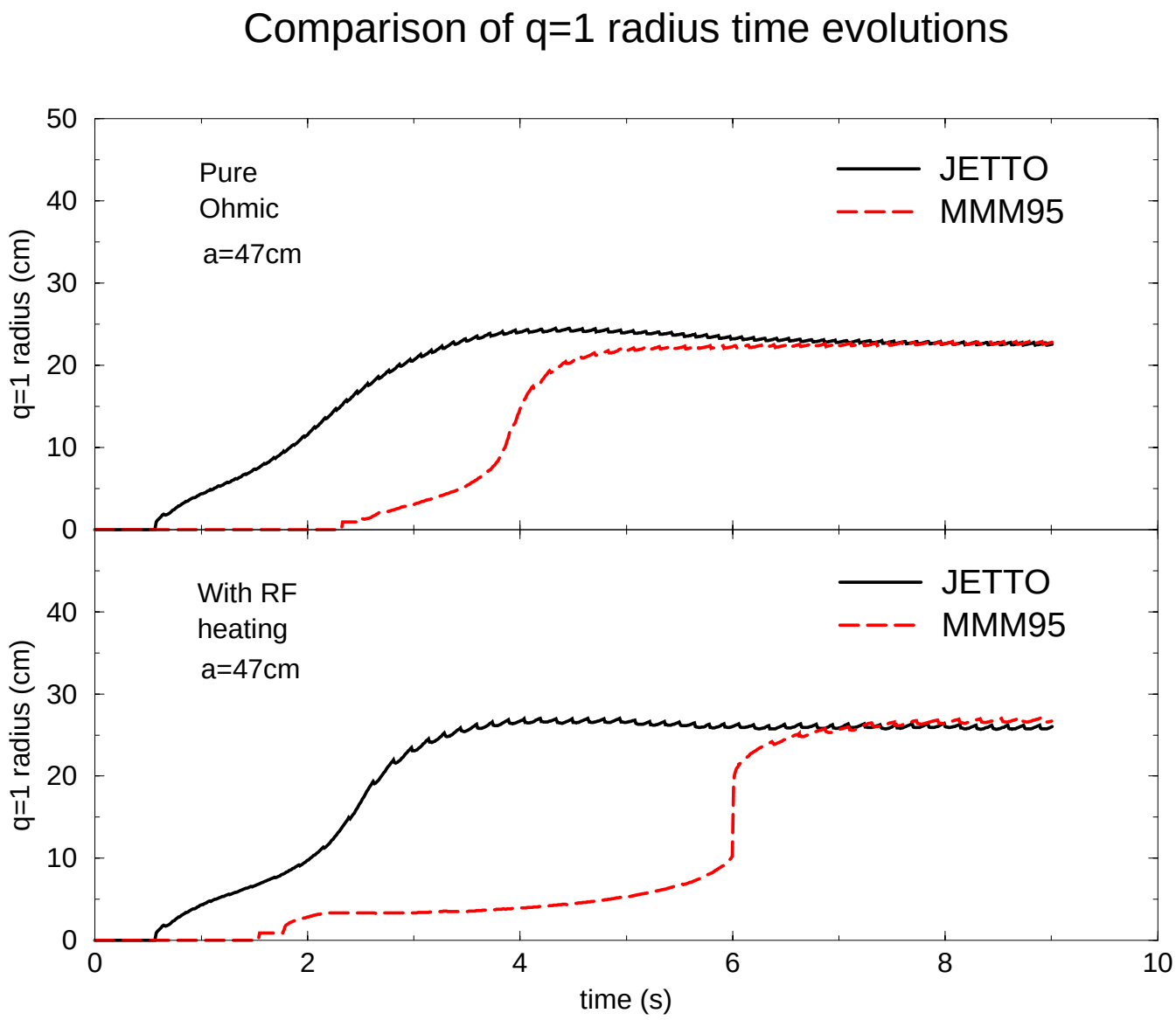
Comparison of q=1 radius time evolutions
Pure
Ohmic
a=47cm
JETTO
MMM95
With RF
heating
a=47cm
JETTO
MMM95
q=1 radius (cm)
q=1 radius (cm)
time (s)
0
10
20
30
40
50
0
2
4
6
8
10

Fig.6

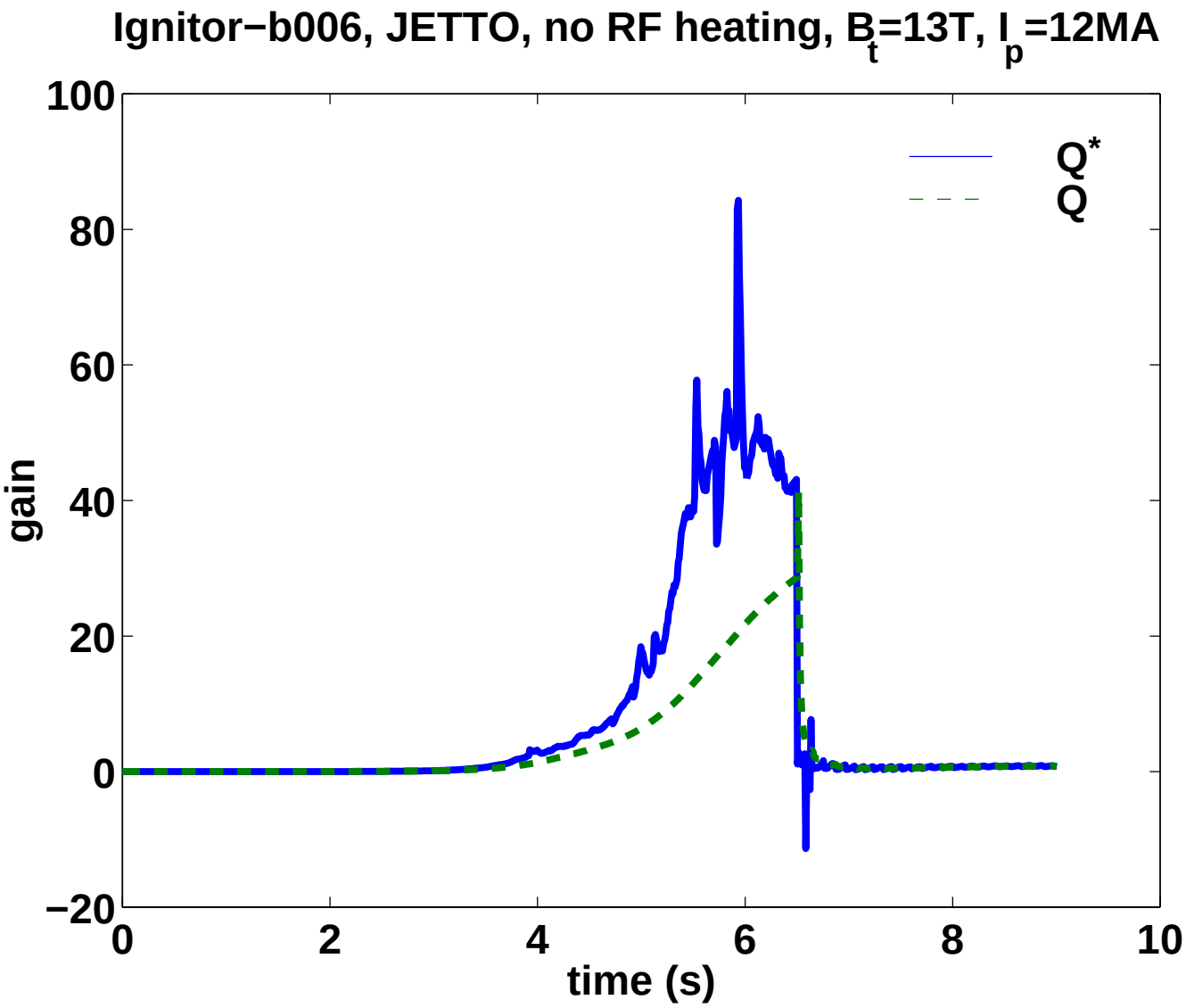
Ignitor−b006, JETTO, no RF heating, B_t=13T, I_p=12MA
100
80
60
40
20
0
−20
gain
0
2
4
6
8
10
time (s)
Q*
Q

Fig.7

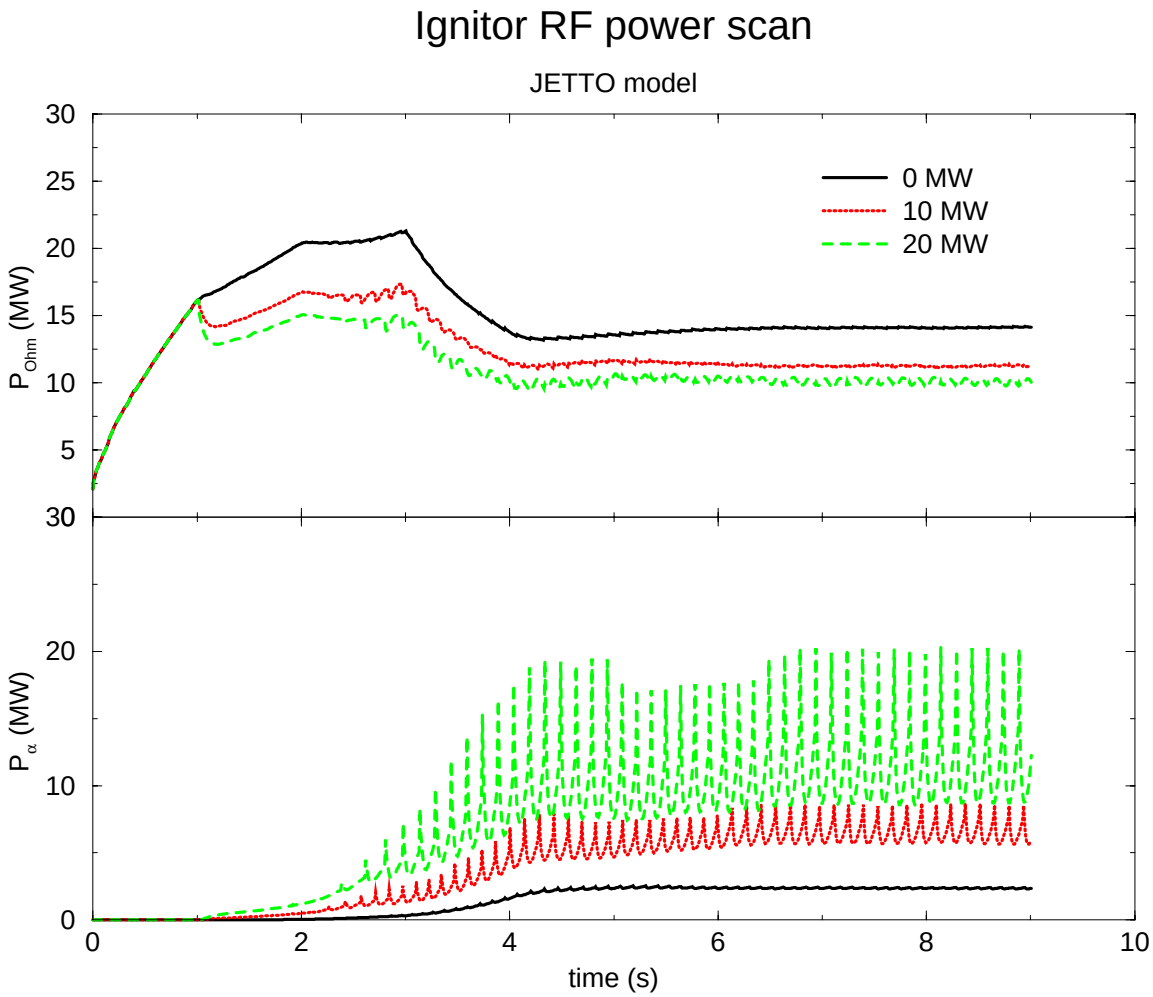
Ignitor RF power scan
JETTO model
0 MW
10 MW
20 MW
P_Ohm (MW)
P_α (MW)
time (s)
0
5
10
15
20
25
30
2
4
6
8

Fig.8

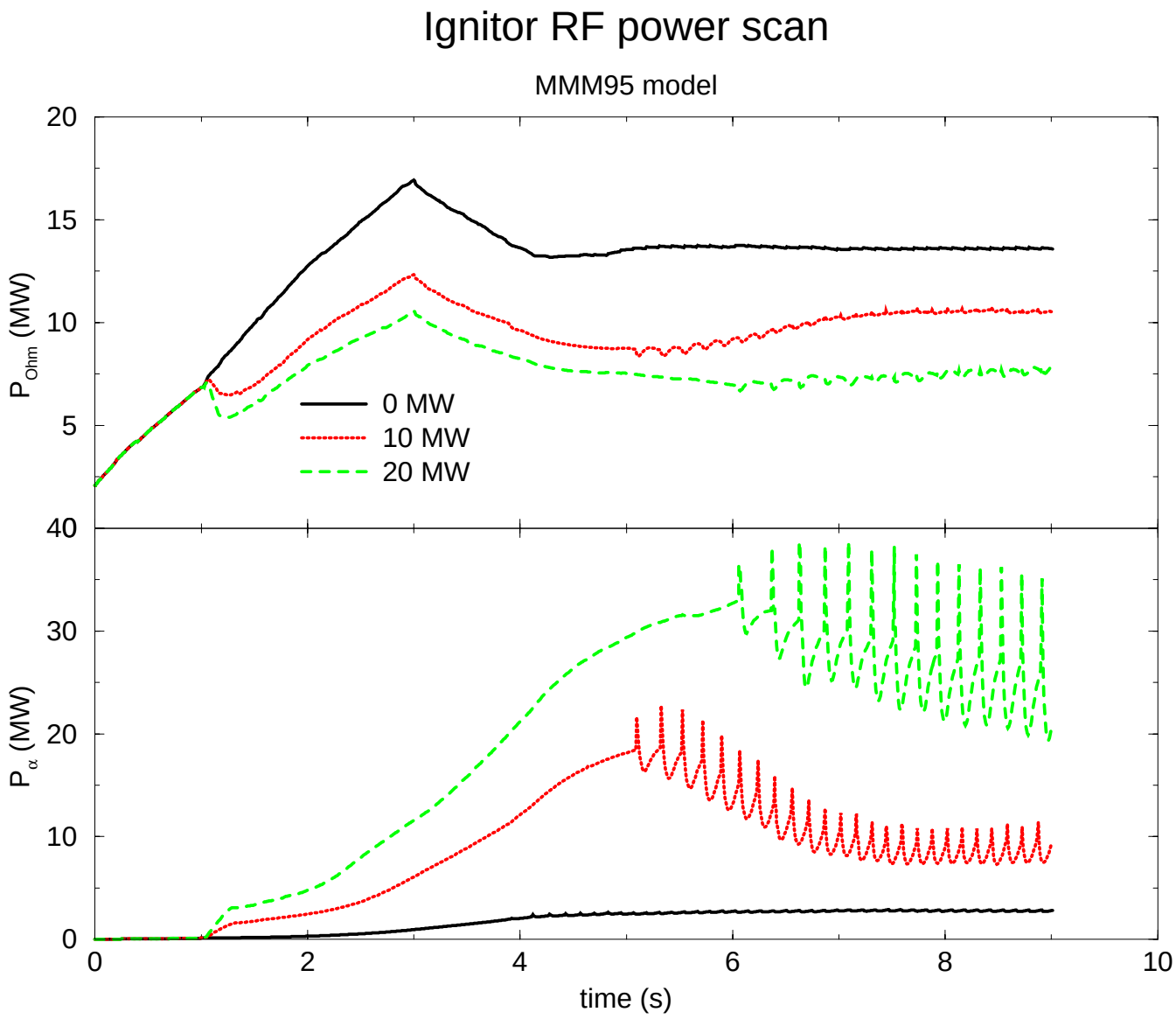
Ignitor RF power scan
MMM95 model
P_Ohm (MW)
P_α (MW)
time (s)
0 MW
10 MW
20 MW
0
5
10
15
20
0
10
20
30
40
0
2
4
6
8
10

Fig.9